



Introducing a New Method for Purification of Human IL-4 by Substitution of a Single Amino Acid in IL-4 Protein Sequence

Mohsen Mazloomrezaei¹, Mahsa Sadat Hosseini¹, Nahid Ahmadi^{1,2}, Elham Mahmoudi Maymand¹, Ebrahim Eftekhari³, Amir Asgari⁴, Amin Ramezani^{1,2*}

¹Shiraz Institute for Cancer Research, School of Medicine, Shiraz University of Medical Sciences, Shiraz, Iran; ²Department of Medical Biotechnology, School of Advanced Medical Sciences and Technologies, Shiraz University of Medical Sciences, Shiraz, Iran; ³Molecular Medicine Research Center, Hormozgan Health Institute, Hormozgan University of Medical Sciences, Bandar Abbas, Iran; ⁴Faculty of Pharmacy and Pharmaceutical Sciences, University of Alberta, Edmonton, Alberta, Canada

ABSTRACT

Background: It is advantageous to develop an effective purification procedure to produce recombinant protein drugs (rPDs) without any tags. To remove N- or C-terminus tags from the rPDs, several cleavage site-based endopeptidases were used. Separating the endopeptidase enzyme from the rPDs is a time-consuming and costly process.

Objective: To design and develop a new method for the purification of human interleukin (IL)-4 with potential application for other cytokines.

Methods: Met-like amino acids were substituted at position 120 to reduce the possibility of alteration in the structure of IL-4 and its biological activity. Based on the *in silico* analysis, isoleucine was chosen as an alternative amino acid, and the M120I mutant IL-4 (mIL-4) model was selected for the downstream analysis. Recombinant mIL-4 was produced in the E.coli BL21 host and purified with CNBr. Then *in vitro* evaluations of the native and mutant IL-4 were performed.

Results: The results showed that both the native and mutant IL-4 had the same effect on TF-1 cell proliferation. On the other hand, there was no significant difference between the effects of native IL-4 (nIL-4) and mIL-4 on the expression of IL-4 and IL-10 in activated peripheral blood mononuclear cells. Native and mutant IL-4 have similar biological activities.

Conclusion: Here, an efficient and straightforward system is introduced to purify IL-4 cytokine using CNBr, which could be applied to other rPDs.

Keywords: Cyanogen Bromide, Interleukin-4, Protein Purification, Tag removal

*Corresponding author:
Amin Ramezani,
Shiraz Institute for Cancer
Research, School of Medicine,
Shiraz University of Medical
Sciences, Shiraz, Iran
Tel/Fax: +98 71 32303687
Email: aramezani@sums.ac.ir

Cite this article as:
Mazloomrezaei M, Hosseini MS,
Ahmadi N, Mahmoudi Maymand
E, Eftekhari E, Asgari A, Ramezani
A. Introducing a New Method for
Purification of Human IL-4 by
Substitution of a Single Amino Acid
in IL-4 Protein Sequence. *Iran J
Immunol.* 2022; 19(4):436-445,
doi: 10.22034/iji.2022.94985.2336.

Received: 2022-03-16
Revised: 2022-06-05
Accepted: 2022-06-27

INTRODUCTION

It is imperative to have an effective purification procedure to produce recombinant protein drugs (rPDs), including monoclonal antibodies, vaccines, and therapeutic proteins on an industrial scale [1]. The cost management in the purification process of recombinant proteins has been thoroughly studied. However, it is still considered a significant cost-bearing step as liquid chromatography is typically used as a core purification method [2]. To address such financial challenges from the pharmacoeconomic perspective, optimization must be adopted to reduce the cost of producing rPD.

The main types of liquid chromatography include affinity, size exclusion, cation exchange, ion exchange, and hydrophobic interaction chromatography. Affinity chromatography with high selectivity or specificity relies on the interaction of the protein with the stationary phase [3]. It can be performed using various ligands, such as immobilized metal ions, borates, lectins, antibodies, and aptamers. As a tool to separate and analyze rPDs in complex samples, affinity chromatography will continue to gain importance and popularity [4].

To improve the purification efficiency, several amino acid tags were designed to bind to the N- or C-terminus of the target protein, and special cleavage site-based endopeptidases were used to remove these tags. Separating the endopeptidase enzyme from the recombinant protein is a relatively difficult and expensive process [5]. Several techniques have been developed to eliminate this difficulty, such as cyanogen bromide (CNBr) cleavage. This chemical is known to hydrolyze the C-terminal amide bonds to Methionine (Met) residues with extremely high efficiency (>90%) [5-8].

Interleukin (IL)-4 is a cytokine that is considered to have a vital role in regulating the immune system. It is believed that IL-4 induces the differentiation of naïve CD4 T cells into T helper type 2 (Th2) cells. IL-4 is

also a favorable therapeutic candidate and is undergoing phases I and II of clinical trials to treat malignancies such as leukemia, non-Hodgkin's lymphoma, acute myelogenous leukemia (AML), and infectious and inflammatory diseases [9-11].

This study aimed to develop the conditions for using CNBr to cleave the N-terminal tags of rPDs. To fulfill this aim, the Met amino acids in the protein sequence should be replaced with other amino acids so that the protein's third structure and biological activity are not affected. For this purpose, the IL-4 protein was chosen, which has only one Met amino acid at position 120 in addition to the initial Met. Using *in silico* approaches, an alternative amino acid was chosen, and after studying the protein's third structure, recombinant mutant IL-4 was produced in the *E. coli* BL21 host and purified with CNBr. *In vitro* experiments were used to compare the physicochemical properties and biological activities of mutant IL-4 (mIL-4) with the native IL-4 (nIL-4).

MATERIALS AND METHODS

In Silico Analysis

The amino acid sequence of IL-4 (P05112) was obtained from the UniProt database (<http://www.uniprot.org/>). Met-like amino acids have been substituted at position 120 to reduce the possibility of alteration in the structure of IL-4 and its biological activity. The ProtParam web server calculated several physicochemical parameters, including molecular weight, theoretical isoelectric point (pI), and the total number of positive and negative residues (<http://us.expasy.org/tools/protparam.html>).

The 3D structure of mIL-4 was predicted based on homology modeling by several algorithms, including I-TASSER online server (<http://zhanglab.cmb.med.umich.edu/I-TASSER>), Phyre2 server (<http://www.sbg.bio.ic.ac.uk/phyre2>) and SWISS-MODEL (<http://swissmodel.expasy.org/>). The

RAMPAGE (<http://mordred.bioc.cam.ac.uk/rapper/rampage.php>), ProSA-web (<https://prosa.services.came.sbg.ac.at/prosa.php>), Verify3D (http://servicesn.mbi.ucla.edu/Verify_y3D/) and ERRAT servers (http://nihserver.mbi.ucla.edu/ERRAT_v2/) were utilized to validate the predicted model. The final model was introduced to the GalaxyRefine server (<http://galaxy.seoklab.org/>) to reconstruct and repack side chains.

The mIL-4 IL-4 receptor alpha interactions were predicted using the SwarmDock algorithm (<http://bmm.crick.ac.uk/~SwarmDock/index.html>).

Native and Mutant IL-4 Protein Production and Purification

The coding sequences that encode native and mutant IL-4 were gene-optimized using GenScript's multiparameter gene optimization algorithm, OptimumGene™. Nucleotide fragments were synthesized by Biomatik in the pBSK vector and amplified using PCR. Amplified genes were then inserted into *NcoI* and *XhoI* restriction sites of a pET28/NT-His vector, resulting in the expression of proteins with a N-terminal histidine (HIS) Tag. Recombinant pET28-IL-4 vectors were then transformed into *E.coli* BL21 competent cells using the Heat Shock method, and overexpression was then induced by 0.25 mM isopropyl β-d-1-thiogalactopyranoside (IPTG) (Fermentas, Lithuania). Cultures were harvested after 24 hrs. and pelleted by centrifugation at 6000 ×g for 15 mins at 4 °C. The cells were then resuspended in Lysis buffer (500 mM NaCl and 20 mM NaH₂PO₄:Na₂HPO₄) and incubated for 45 mins at 4 °C with 1 mg/ml Lysozyme (Sigma, USA). Several freeze-thaw cycles were applied to increase the lysis efficiency. 2% sarkosyl (Sigma, USA) was added to the cell lysate suspension and incubated for two hrs. on the shaker at room temperature to solubilize inclusion bodies. The lysate was then centrifuged at 4 °C for 30 mins at 13,000 ×g to recover the supernatant containing the solubilized protein. The

Ni-NTA resin was used for IL-4 protein purification according to Asgari et al. (2019), and protein concentration was determined by LEGEND MAX™ human il-4 ELISA kit according to the manufacturer's instruction (BioLegend, CA, USA) [12].

Purified mIL-4 was dissolved in a solution containing formic acid, water, and CNBr, and incubated at room temperature. After 24 hrs., sodium hydroxide was used to neutralize CNBr, and mIL-4 protein was purified using a G25 desalting column. The purified nIL-4 was used in all experimental tests to compare with mIL-4.

In vitro Evaluation of Native and Mutant IL-4 Physicochemical Analysis

The Western blotting was used to confirm the native and mutant IL-4 protein size. Briefly, purified native and mutant IL-4 proteins were separated by 12.5% SDS-PAGE and then transferred to a PVDF membrane (Thermo Fisher Scientific, USA). The membrane was incubated with mouse anti-human IL-4 antibody (Abcam, USA) as a primary antibody and then with horseradish peroxidase-conjugated goat anti-mouse IgG (Abcam, USA) as a secondary antibody. Enhanced chemiluminescence (ECL) (Bio-Rad, USA) was used to detect the peroxidase activity. Commercially available recombinant human IL-4 (Biolegend, San Diego, CA) and recombinant GFP produced in *E.coli* were used as the positive and negative controls, respectively.

Proliferation Assay

The proliferation effect of native and mutant IL-4 on TF-1 cell line (Erythroleukemic) was evaluated with 3-(4,5-dimethylthiazol-2-yl)-2,5-diphenyltetrazolium bromide (MTT) assay. TF-1 was prepared by the National Cell Bank of Iran (Pasteur Institute, Iran) and was maintained in the RPMI 1640 supplemented with 10% FBS. 2×10⁴ cells per well were seeded into 96-well plates and incubated overnight (approx. 16 hrs.) at 37 °C, 5% CO₂. Then, the 50µl of fresh media containing

different concentrations of native and mutant IL-4 as well as commercially available recombinant human IL-4 (0, 0.0001, 0.001, 0.01, 0.1, 1, and 10 ng/ml) were added to each well. The plates were then incubated for 48 hrs. at 37 °C in a 5% CO₂ incubator. Each well received a 0.5mg/ml final concentration of tetrazolium bromide solution (Sigma, USA) and was incubated for 4 hrs. After aspirating the media from each well, 150 µl dimethyl sulfoxide (DMSO) was added to dissolve the formazan crystals. A microplate reader was used to measure absorbance at 570 nm. All of the experiments were carried out in triplicates. Effective dose 50 (ED50) was calculated using “Quest Graph™ ED50 Calculator” (“Quest Graph™ ED50 Calculator.” AAT Bioquest, Inc, 19 Apr. 2021, <https://www.aatbio.com/tools/ed50-calculator>).

Quantitative real-time Polymerase Chain Reaction (qRT-PCR) Analysis

Six healthy donors provided five milliliters of whole blood to isolate peripheral blood mononuclear cells (PBMCs) using a Ficoll-Paque density gradient centrifuge. All the donors provided written informed consent before participating in this study. The phytohemagglutinin (PHA)-activated PBMCs were cultured in 24-well plates with different concentrations of rhIL-4, nIL-4, and mIL-4 for 24 hrs. For each protein, three different concentrations, including 1/2×ED50, ED50, and 2×ED50 were used. Non-treated PHA-activated PMBC was used as the control for data normalization. Total cellular RNA was isolated from 3×10⁵ cells using the RNXplus reagent (CinnaGen, Iran). Next, 1µg of DNase-treated RNA was used for the first-strand cDNA synthesis using ThermoScientific RevertAid First Strand cDNA Synthesis Kit in a 20µl final volume. TaqMan primer and probe design were carried out using Allele ID 7 software for the human IL-10, IL-4, and β Actin genes. Relative real-time PCR was performed in a 20µl volume by TaqMan Universal PCR Master Mix (ABI, London, UK). Ct values were normalized using the

CtNorm algorithm, and differences in gene expression were calculated against β Actin as a housekeeping gene via the ABI StepOne Real-Time PCR (Applied Biosystems, USA) [13, 14]. All amplification reactions were repeated twice under identical conditions.

Data Analysis and Statistics

SPSS software version 20.0 was used to conduct the statistical analysis (IBM Corporation, Armonk, NY, USA). The differences between the groups were assessed using the Kruskal-Wallis statistical test. In addition, the Mann-Whitney U test was employed for comparisons between the study groups or different samples. All data are presented as the mean±SEM, and significant differences were defined as *p*-values equal to or less than 0.05 (*P*≤0.05). The software GraphPad Prism 6 was used to construct each graph (GraphPad Software, San Diego, CA).

RESULTS

In Silico Analysis

According to the Venn diagram, seven Met-like amino acids were selected to substitute at position 120: Leucine (Leu), Isoleucine (Ile), Valine (Val), Tyrosine (Tyr), Phenylalanine (Phe), Alanine (Ala), Histidine (His), and Tryptophan (Trp) [15].

The mIL-4 protein contained 129 amino acids, with 21 positively charged (Arg, Lys) and 14 negatively charged (Asp, Glu) residues. The described construct had a molecular weight (MW) of about 17 kDa and an pI of 9.17.

To predict the 3D model of each protein, the SWISS-MODEL, I-TASSER, and PHYER2.0 Server homology modeling approaches were used. The top models in the Swiss model server were chosen based on their GMQE and QMEAN Z score values. The depicted ‘good’ models achieve QMEAN Z-scores comparable with the experimental structures (the mean Z-score=-0.65), while the ‘medium’ quality models fall somewhere in the middle (the mean Z-score=-1.75) [16].

Based on the root mean square deviation (RMSD), template modeling score (TM-score), Z-score, Ramachandran values, and VERIFY3D and ERRAT scores, the SWISS model with isoleucine substitution (M120I) was chosen as the mutant IL-4 model for the downstream analysis. This model was presented to the GalaxyRefine server for refinement, and a model with a -6.21 z-score was achieved. The RAMPAGE server reported that 98.5%, 1.5%, and 0.0% of the refined model's residues were located in favored, allowed, and outlier regions, respectively.

The ribbon diagram of the IL-4 (1BCN) and the predicted structure of the final model of mIL-4 (M120I) generated by SWISS-MODEL are shown in Figures 1a and 1b, respectively. The superimposition of modeled mIL-4 (M120I) on IL-4 (1BCN) as a template showed a high degree of agreement in four major helices (Figure 1c).

SwarmDock, a protein-protein docking server, allows researchers to discover the most relevant regions of mIL-4 (M120I) interacting with IL-4R α . Figure 2 depicts the greatest refined model of the ligand and receptor complex, with a global energy value of -30.10 kcal/mol, and the interaction

complex of mIL-4 (M120I) and IL-4R α .

Native and Mutant IL-4 Protein Production

The correctness of the nucleotide sequences of native and mutant IL-4 cloned in the pET28 plasmid was confirmed by sequencing results. The purified native and mutant IL-4 yields were estimated to be around 43.1 mg/l and 38.5 mg/l, respectively, using an ELISA assay. Furthermore, the western blot confirmed the presence of both the native and mutant IL-4, as well as its size similarity to commercially available recombinant human IL-4 (Figure 3).

TF-1 Cell Lines Proliferation in Response to Native and Mutant IL-4

The MTT test was used to assess the proliferation effect of both the native and mutant IL-4 on TF-1 cells. Figure 4 illustrates that the native and mutant IL-4 had similar effects on TF-1 cell proliferation (ED50: 0.026 and ED50: 0.023, respectively) as compared with the effect of commercially available recombinant human IL-4 as a positive control (ED50: 0.029).

IL-4 Stimulates PBMCs to Produce More IL-4 and IL-10

We expanded our research by investigating

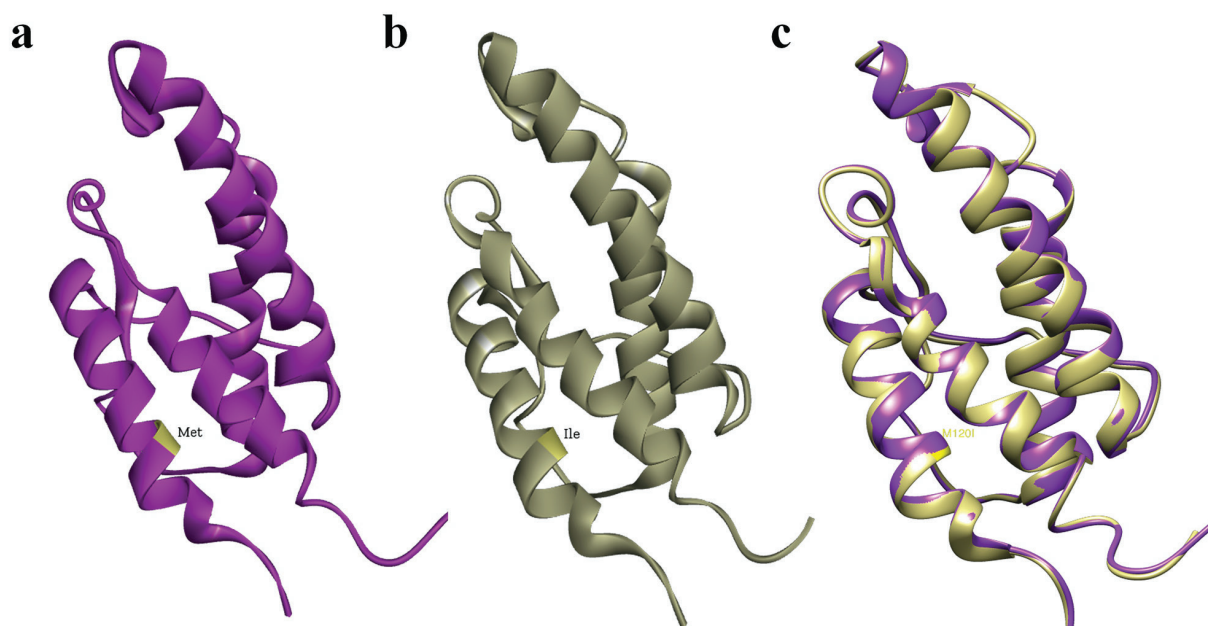


Figure 1. Structure modeling 3D presentation of the IL-4 (1BCN) as the template (a). The final model of mIL-4 (M120I), generated by SWISS-MODEL. M120I Position is highlighted in yellow (b). Superimposed structure of template (purple colored) and homology model of mIL-4 (M120I) (gray colored) (c). The molecular graphic images were produced using the UCSF Chimera package

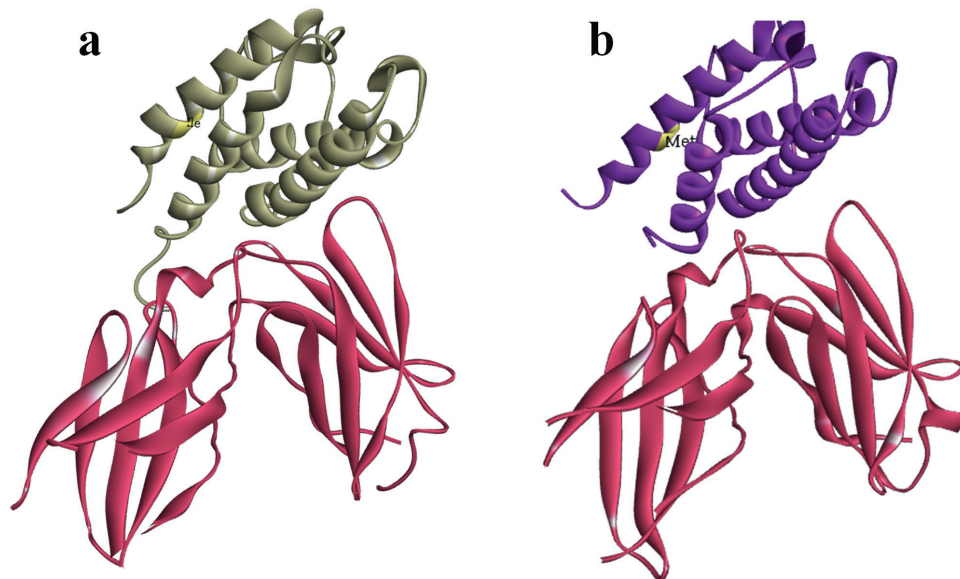


Figure 2. Docking results for protein-protein interactions between (a) mIL-4 (M120I)–IL-4R α and (b) hIL-4–IL-4R α . The UCSF Chimera package was used to visualize the docked structures

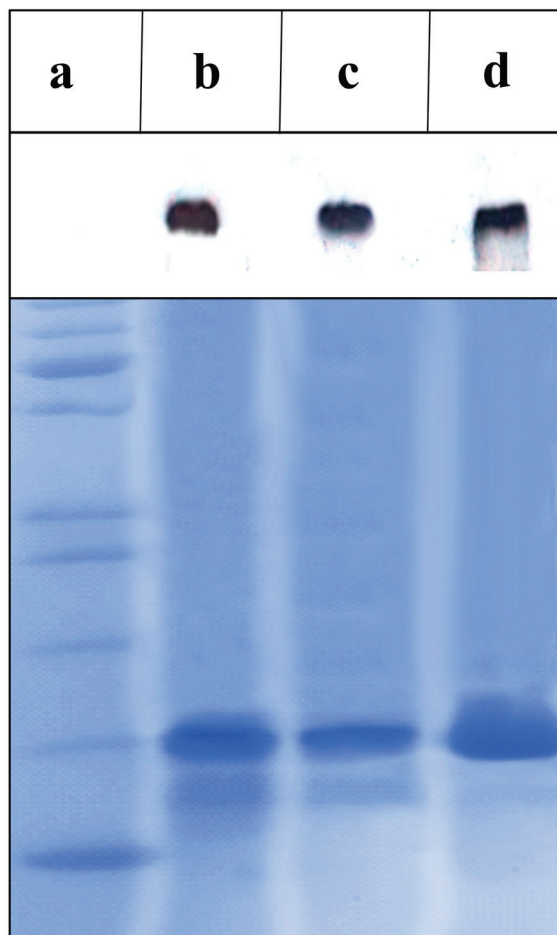


Figure 3. Native and mutant IL-4 purity and size evaluation using SDS-PAGE and the Western blotting. Four fractions denoted protein molecular marker (a), purified mIL-4 (b), purified nIL-4 (c), and commercially available recombinant human IL-4 (d).

how rhIL-4, nIL-4, and mIL-4 influence IL-4 and IL-10 expression in activated PBMCs. For each protein, three different concentrations were used: $1/2 \times \text{ED}_{50}$, ED_{50} , and $2 \times \text{ED}_{50}$, and as illustrated in Figures 5a and 6a, none of the three proteins showed a statistically significant difference. IL-4 and IL-10 expression, on the other hand, increased significantly in response to increasing concentrations of rhIL-4, nIL-4, and mIL-4 (Figures 5b and 6b). However, high concentrations of IL-4 (ED_{50} and $2 \times \text{ED}_{50}$) have a more significant effect on IL-4 expression than on IL-10 expression.

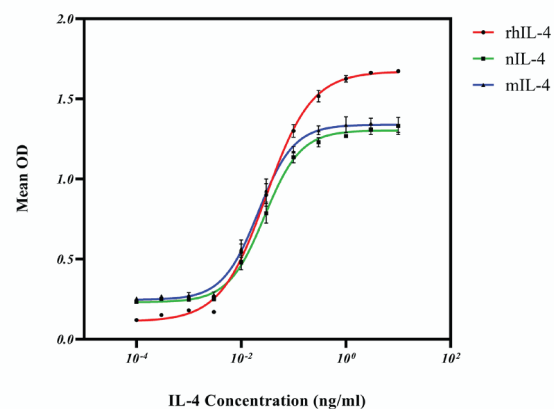


Figure 4. Proliferation induction of rhIL-4, nIL-4 and mIL-4 on TF-1 cells. IL-4 concentrations greater than 10^{-3} ng/ml significantly increased TF-1 cell proliferation. rhIL-4 ED_{50} : 0.029, nIL-4 ED_{50} : 0.026, and mIL-4 ED_{50} : 0.023

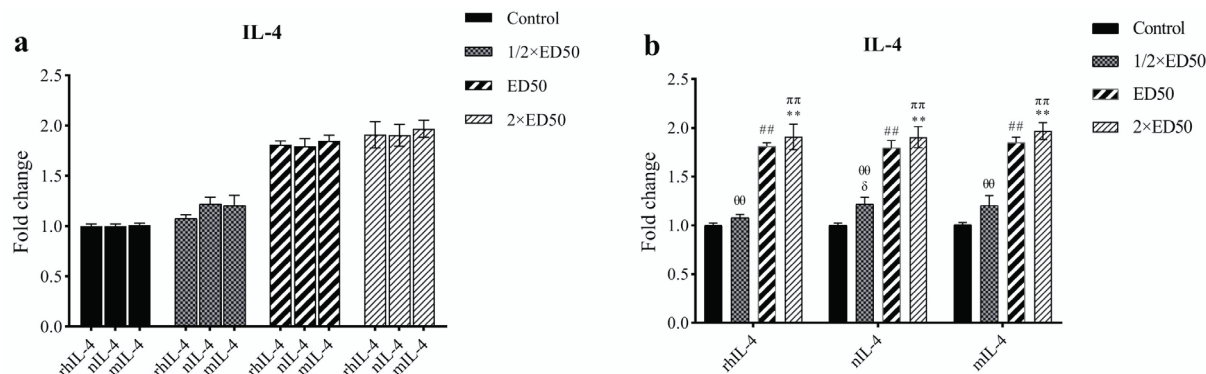


Figure 5. IL-4 induces IL-4 production in PBMCs. The effect of rhIL-4, nIL-4, and mIL-4 at different concentrations (1/2×ED50, ED50, and 2×ED50) on IL-4 expression in PBMCs is compared. a) Each group contained three proteins at the same concentration, and there was no statistically significant difference within each group ($P \geq 0.05$). b) Each group had four different concentrations of each protein, and as can be seen, IL-4 expression increased significantly as rhIL-4, nIL-4, and mIL-4 concentrations increased ($P \leq 0.01$). Error bars show the mean \pm SEM. The Mann-Whitney U test determined the statistical significance. The statistically significant difference between δ) the control and 1/2×ED50 groups, #) the control and ED50 groups, *) the control and 2×ED50 groups, θ) the 1/2×ED50 and ED50 groups, and π) the 1/2×ED50 and 2×ED50 groups

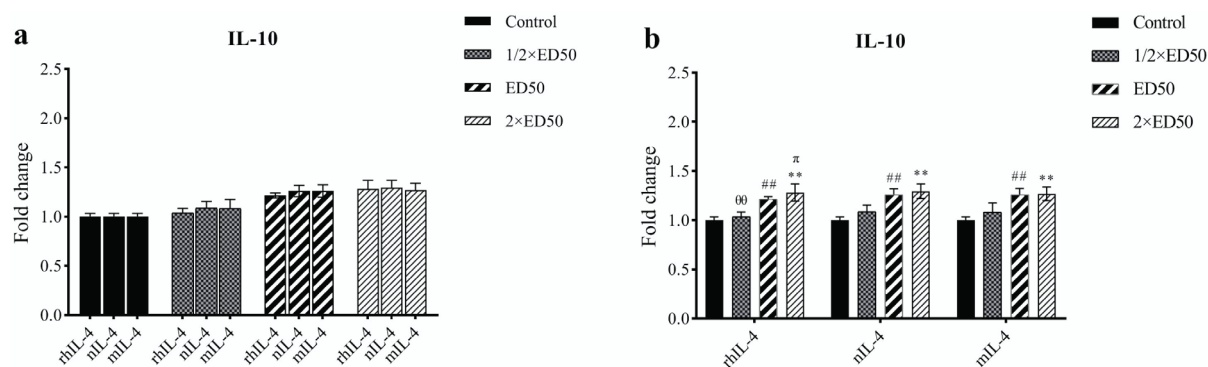


Figure 6. IL-4 stimulates the production of IL-10 in PBMCs. The effect of rhIL-4, nIL-4, and mIL-4 on IL-10 expression in PBMCs is compared at different concentrations (1/2×ED50, ED50, and 2×ED50). a) Each group had three proteins at the same concentration, and there was no statistically significant difference within each group ($P \geq 0.05$). b) Each group contained four different concentrations of each protein, and as can be seen, IL-10 expression increased significantly as rhIL-4, nIL-4, and mIL-4 concentrations increased ($P \leq 0.01$). Error bars show the mean \pm SEM. The Mann-Whitney U test determined the statistical significance. The statistically significant difference between δ) the control and 1/2×ED50 groups, #) the control and ED50 groups, *) the control and 2×ED50 groups, θ) the 1/2×ED50 and ED50 groups, and π) the 1/2×ED50 and 2×ED50 groups

DISCUSSION

Effective purification techniques and high-yield expression hosts are required for efficient recombinant protein production [17]. Compared with other methods used for this purpose, affinity purification has some advantages [18]. Recently, different fusion tags have been developed to improve the detection or purification, tag removal, and solubility of recombinant proteins. Histidine tags have been the most commonly used of all tags since they

are less disruptive, less immunogenic, and have a higher recovery rate than the other tags [19].

The fusion tags should not affect the biological function or folding of the purified protein, and in some cases, they should be removed after purification. To remove fusion tags, chemical techniques such as CNBr and hydroxylamine and enzymatic methods have been developed [18]. However, while the enzymatic strategy can rapidly purify recombinant proteins, the final product almost always contains several amino acids, and

the proteolytic enzyme contaminates them, too, which may affect the activity or cause unwanted immune responses in humans. Furthermore, enzymatic cleavage is costly and unsuitable for large-scale protein production; therefore, less expensive methods are required [20]. Chemical cleavage with CNBr not only does not result in unspecific degradation, but is also inexpensive and suitable for an industrial-scale production [21].

The purpose of this experiment was to purify the IL-4 protein using CNBr. To accomplish this purpose, the Met amino acid at position 120 must be replaced with other amino acids so that CNBr cleavage does not fragment the IL-4 protein. This limitation is most likely to be overcome by replacing Met-120 with Ile, Leu, Val, Phe, Ala, Tyr, His, and Trp, which are all conservative changes. According to the *in silico* modeling results, Ile was the best alternative to Met-120, which did not significantly alter the properties of recombinant IL-4. The 3D structure of mIL-4 (M120I) was predicted using the homology modeling approach, and validation calculations confirmed the high quality of the modeled protein created by SWISS-MODEL. Docking results revealed that mIL-4 (M120I) interacts with IL-4R α in the same way the nIL-4 does.

Several expression systems have been used to produce recombinant IL-4, and it has been reported that recombinant IL-4 produced in *E. coli* is both immunologically and biologically active [22, 23]. In this study, IL-4 was produced in *E. coli*, and 2% sarkosyl, an anionic detergent, was employed to solubilize the protein in inclusion bodies. Following the solubilization, the IL-4-containing supernatant was directly added to the Ni-NTA column to purify the His-tagged protein. The cytokine IL-4 contains three disulfide bonds, and its activities are known to be disulfide bond-dependent. Other studies and businesses, too, use *E. coli* as a host to produce IL-4 protein.

The MTT assay confirmed that mIL-4, like nIL-4, has a significant effect on TF1 cell

proliferation at concentrations greater than 10^{-3} ng/ml, however, the pattern of cell proliferation is similar. Although TF-1 cells depend on GM-CSF, they can proliferate in response to IL-4 and IL-13, making them an ideal model for studying the IL-4/IL-13 receptor system. This well-established effect of IL-4 was used to validate the function of mIL-4 [24].

We investigated the effects of rhIL-4, nIL-4, and mIL-4 on IL-4 and IL-10 expression in activated PBMCs. IL-4 and IL-10 production increased at three different concentrations of each protein. We concluded that IL-4 increases IL-4 and IL-10 production in activated PBMCs, controlling the ratio of pro-inflammatory to anti-inflammatory cytokines. In LPS-stimulated macrophages, Cao et al. (2005) discovered that IL-4 increases the expression of IL-10 [25]. IL-10, an immunomodulatory cytokine, is essential for maintaining homeostasis and, in particular, controlling immunopathology in autoimmune, infectious, and allergic diseases [26]. There is no significant difference between the effects of nIL-4 and mIL-4 on the expression of IL-4 and IL-10 in activated PBMCs, indicating that they have similar biological activities.

In the light of the high expression levels obtained in different systems and the simple affinity purification protocols available, tag removal is essential in producing rPDs to prevent immunological responses in humans. Combining CNBr cleavage and Met insertion were presented for long synthetic peptides, which could potentially be appropriate for any rPDs production system [20]. Here, we introduced this efficient and straightforward system to purify IL-4 cytokine, which could also purify other recombinant proteins. A simple chemical cleavage reaction and standard affinity chromatography can achieve such specific recovery of an rPD.

ACKNOWLEDGMENTS

This work was supported by the Shiraz University of Medical Sciences (Grant No.

13103), and Shiraz Institute for Cancer Research (Grant No. ICR-100-509). The study was approved by the Research Ethics Committee of Shiraz University of Medical Sciences (Approval ID: IR.SUMS.REC.1396.S892).

Conflict of Interest: None declared.

REFERENCES

- An, J., S. Kim, A. Shrinidhi, J. Kim, H. Banna, G. Sung, K.M. Park, and K. Kim. Purification of protein therapeutics via high-affinity supramolecular host-guest interactions. *Nat Biomed Eng.* 2020; 4(11): p. 1044-1052.
- Schillberg, S., N. Raven, H. Spiegel, S. Rasche, and M. Buntru. Critical analysis of the commercial potential of plants for the production of recombinant proteins. *Front Plant Sci.* 2019; 10: p. 720.
- Geng, X. and L. Wang. Liquid chromatography of recombinant proteins and protein drugs. *J Chromatogr B Analyt Technol Biomed Life Sci.* 2008; 866(1): p. 133-153.
- Hage, D.S., J.A. Anguizola, C. Bi, R. Li, R. Matsuda, E. Papastavros, E. Pfaunmiller, J. Vargas, and X. Zheng. Pharmaceutical and biomedical applications of affinity chromatography: recent trends and developments. *J Pharm Biomed Anal.* 2012; 69: p. 93-105.
- Pane, K., L. Durante, E. Pizzo, M. Varcamonti, A. Zanfardino, V. Sgambati, A. Di Maro, A. Carpentieri, V. Izzo, and A. Di Donato. Rational design of a carrier protein for the production of recombinant toxic peptides in *Escherichia coli*. *PLoS One.* 2016; 11(1): p. e0146552.
- Gross, E. and B. Witkop. Nonenzymatic cleavage of peptide bonds: the methionine residues in bovine pancreatic ribonuclease. *J Biol Chem.* 1962.
- Hwang, P.M., J.S. Pan, and B.D. Sykes. Targeted expression, purification, and cleavage of fusion proteins from inclusion bodies in *Escherichia coli*. *FEBS Lett.* 2014; 588(2): p. 247-252.
- Maicas, S., I. Moukadiri, A. Nieto, and E. Valentin. Construction of an expression vector for production and purification of human somatostatin in *Escherichia coli*. *Mol Biotechnol.* 2013; 55(2): p. 150-158.
- Majhail, N.S., M. Hussein, T.E. Olencki, G.T. Budd, L. Wood, P. Elson, and R.M. Bukowski. Phase I trial of continuous infusion recombinant human interleukin-4 in patients with cancer. *Invest New Drugs.* 2004; 22(4): p. 421-426.
- Lundin, J., E. Kimby, L. Bergmann, T. Karakas, H. Mellstedt, and A. Österborg. Interleukin 4 therapy for patients with chronic lymphocytic leukaemia: a phase I/II study. *Br J Haematol.* 2001; 112(1): p. 155-160.
- Vokes, E.E., R. Figlin, H. Hochster, M. Lotze, and M.E. Rybak. A phase II study of recombinant human interleukin-4 for advanced or recurrent non-small cell lung cancer. *Cancer J Sci Am.* 1998; 4(1): p. 46-51.
- Asgari, A., S. Sharifzadeh, A. Ghaderi, A. Hosseini, and A. Ramezani. In vitro cytotoxic effect of Trastuzumab in combination with Pertuzumab in breast cancer cells is improved by interleukin-2 activated NK cells. *Mol Biol Repts.* 2019; 46(6): p. 6205-6213.
- Ramezani, A. CtNorm: Real time PCR cycle of threshold (Ct) normalization algorithm. *J Microbiol Methods.* 2021; 187: p. 106267.
- Shaaban, Z., M.R. Jafarzadeh Shirazi, M.H. Nooranizadeh, A. Tamadon, F. Rahmanifar, S. Ahmadloo, A. Ramezani, M. Javad Zamiri, I. Razeghian Jahromi, F. Sabet Sarvestani, and O. Koochi Hosseinabadi. Decreased Expression of Arginine-Phenylalanine-Amide-Related Peptide-3 Gene in Dorsomedial Hypothalamic Nucleus of Constant Light Exposure Model of Polycystic Ovarian Syndrome. *Int J Fertil Steril.* 2018; 12(1): p. 43-50.
- Melo, F. and E. Feytmans. Assessing protein structures with a non-local atomic interaction energy. *J Mol Biol.* 1998; 277(5): p. 1141-1152.
- Benkert, P., M. Biasini, and T. Schwede. Toward the estimation of the absolute quality of individual protein structure models. *Bioinformatics.* 2011; 27(3): p. 343-350.
- Healthcare, G. Recombinant protein purification handbook: Principles and methods. GE Healthcare Bio-Sciences AB. 2007.
- Mahmoodi, S., M. Pourhassan-Moghaddam, D.W. Wood, H. Majdi, and N. Zarghami. Current affinity approaches for purification of recombinant proteins. *Cogent Biol.* 2019; 5(1): p. 1665406.
- Manjasetty, B.A., A.P. Turnbull, S. Panjekar, K. Büssow, and M.R. Chance. Automated technologies and novel techniques to accelerate protein crystallography for structural genomics. *Proteomics.* 2008; 8(4): p. 612-625.
- Rais-Beghdadi, C., M.A. Roggero, N. Fasel, and C.D. Reymond. Purification of recombinant proteins by chemical removal of the affinity tag. *Appl Biochem Biotechnol.* 1998; 74(2): p. 95-103.
- Fairlie, W.D., A.D. Uboldi, D.P. De Souza, G.J. Hemmings, N.A. Nicola, and M. Baca. A fusion protein system for the recombinant production of

- short disulfide-containing peptides. *Protein Expr Purif.* 2002; 26(1): p. 171-178.
22. Hatami, H., M. Moghadam, and M. Sankian. Design and Synthesis of Recombinant Murine Interleukin 4 (IL-4). *Arch Pharm Pract.* 2020; 1: p. 46.
 23. Luo, X.-L., X.-X. Ren, N.-Y. Huang, J. Qiu, Q. Li, X.-K. Zhou, and J. Li. The construction of recombinant mouse interleukin 4 prokaryotic expressing plasmid and the expression and purification of target protein. *Sichuan Da Xue Xue Bao Yi Xue Ban.* 2009; 40(4): p. 579-583.
 24. Keegan, A.D., J.A. Johnston, P.J. Tortolani, L.J. McReynolds, C. Kinzer, J.J. O'Shea, and W.E. Paul. Similarities and differences in signal transduction by interleukin 4 and interleukin 13: analysis of Janus kinase activation. *Proc Natl Acad Sci U S A.* 1995; 92(17): p. 7681-7685.
 25. Cao, S., J. Liu, L. Song, and X. Ma. The protooncogene c-Maf is an essential transcription factor for IL-10 gene expression in macrophages. *J Immunol.* 2005; 174(6): p. 3484-3492.
 26. Saraiva, M. and A. O'garra. The regulation of IL-10 production by immune cells. *Nat Rev Immunol.* 2010, 10(3): p. 170-181.